THE JOURNAL OF PHYSICAL CHEMISTRY C

Article

pubs.acs.org/JPCC

Ligand Exchange Reaction on $Au_{38}(SR)_{24}$, Separation of $Au_{38}(SR)_{23}(SR')_1$ Regioisomers, and Migration of Thiolates

Lule Beqa,[†] Damien Deschamps,[‡] Stéphane Perrio,[‡] Annie-Claude Gaumont,[‡] Stefan Knoppe,[†,§] and Thomas Bürgi*[,†]

[†]Department of Physical Chemistry, University of Geneva, 30 Quai Ernest-Ansermet, 1211 Geneva 4, Switzerland

[‡]Laboratoire de Chimie Moléculaire et Thioorganique, UMR CNRS 6507, INC3M, FR 3038, ENSICAEN and Université de Caen Basse-Normandie, 14050 Caen, France

Supporting Information

ABSTRACT: The ligand exchange reaction between $Au_{38}(2\text{-PET})_{24}$ (2-PET: 2-phenylethanethiolate) clusters and enantiopure planar chiral [2.2]paracyclophane-4-thiol **1** (PCP-4-SH) was studied using high performance liquid chromatography (HPLC) and mass spectrometry. It is shown that even at the initial stage of the reaction at least three out of the four symmetry-unique sites are exchanged leading to different regioisomers of composition $Au_{38}(2\text{-PET})_{23}(PCP\text{-}4\text{-}S)_1$. Using HPLC it was possible to isolate one specific regioisomer. The latter is stable at room temperature and at slightly elevated temperatures. However, at 80 °C the adsorbed thiolate (PCP-4-S) moves between different symmetry-unique sites. These observations have implications for the preparation of mixed ligand shell clusters with specific ligand patterns.

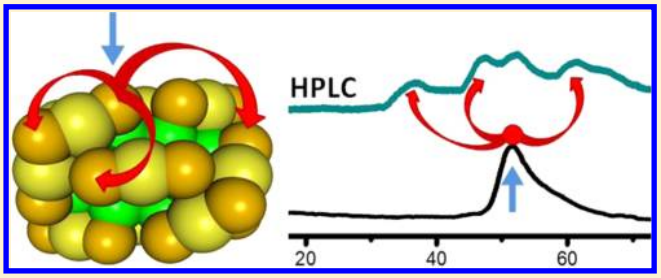

INTRODUCTION

Gold nanoparticles and clusters protected by thiolates are currently in the focus of interest due to their size-dependent optical, electronic, magnetic, and chemical properties,[1−3] which form the basis for applications in fields such as catalysis,[4] sensing,[5] or nanomedicine.[6] Very recently, the field has tremendously progressed due to significant advances in the preparation and characterization of pure cluster compounds of different sizes.[7−9] Also, the structure of several such clusters is now solved.[10−12]

The structure of the gold−sulfur interface of thiolate-protected clusters is characterized by monomeric (SR)-Au-(SR) and dimeric (SR)-Au-(SR)-Au-(SR) staple units. The discovery of these units by X-ray structure determination[10] forms a solid basis for the design and interpretation of surface chemical reactions on thiolate-protected gold clusters and particles. For example, thiolate-for-thiolate exchange reactions are a straightforward method to change the chemical properties of gold nanoparticles or clusters and to add functionality to these nano-objects.[13−15] Ligand exchange can be used for example to change the solubility of the nanoparticles, to induce their self-assembly[16,17] or to introduce functional molecules.[18]

Despite the importance of this versatile chemical reaction not much molecular level information has been deciphered up to now. The extent of thiolate-for-thiolate ligand exchange, which can be determined by thermogravimetric (TG) methods[19] or nuclear magnetic resonance (NMR) spectroscopy,[20,21] can be controlled by varying the reaction time, temperature, and concentration of the cluster and the incoming thiol. TG and NMR yield the *average* number of exchanged ligands. Mass spectrometry, in addition, gives information on the distribution of exchange products.[22−24] Typically, several exchange products with different composition (and therefore different mass) coexist in solution corresponding to species with different numbers of ligands exchanged.[22,25] The ligand exchange reaction is usually fast initially and then slows down considerably.[13] The reaction is thought to proceed via an associative (S_N2-like) mechanism.[15,20,21] Recently, Ackerson and colleagues presented a detailed experimental and computational study on the ligand exchange on the $Au_{102}(p\text{-MBA})_{44}$ cluster (*p*-MBA = *para*-mercaptobenzoic acid).[15] They exchanged a few *p*-MBA ligands by *p*-BBT ligands (*p*-BBT = *para*-bromobenzenethiol) and crystallized the partially exchanged products. They found that 2 out of the 22 symmetry-unique *p*-MBA ligand sites were preferentially exchanged at the initial stage of the reaction. As judged from the partial Br occupancy in the heterogeneous crystal, about 50 and 60%, respectively, were exchanged at these two positions. Interestingly, the two exchanged ligands are bound to solvent accessible Au atoms in agreement with an associative S_N2 mechanism. Although the possibility of selective crystallization of particular ligand exchange products remains, this elegant study seems to indicate that a selective functionalization of the ligand shell of such nanoscale objects is possible. However, even the crystals of ligand exchange products mentioned above

Received: August 23, 2013
Revised: September 13, 2013
Published: September 18, 2013

dx.doi.org/10.1021/jp408455x | J. Phys. Chem. C 2013, 117, 21619−21625

contain a mixture of exchange species with different number of exchanged ligands and/or different exchange positions.[15]

Negishi and co-workers recently reported the separation of ligand exchange products with different composition $PdAu_{24}(SR)_{18-n}(SR')_n$ (n = 0, 1, 2, ..., 18) by gradient elution HPLC, making use of the different solubility of the two ligands.[23] It is important to note that within such a fraction a large number of regioisomers can coexist, differing only in the position of the exchanged ligands on the cluster. Some of the peaks in the HPLC chromatograms reported in ref 23 are indeed asymmetric, which could be due the coexistence of isomers.

Similarly, we separated Au_{38} clusters exchanged with one or two axially chiral BINAS dithiol ligands (BINAS = 1,1′-binaphthyl-2,2′-dithiol) by (chiral) HPLC. The peak in the HPLC was well-defined and we argued that the rigid dithiol selectively exchanges at one site only.[26] We have also shown recently that the chiral $Au_{38}(2\text{-PET})_{24}$ cluster can undergo racemization at moderate temperatures,[27] which was shifted to higher temperatures upon introducing one BINAS ligand.[28] Racemization implies that several dimer (SR)-Au-(SR)-Au-(SR) units rearrange on the cluster surface, which reveals the flexibility of the gold−thiolate interface.

The $Au_{38}(SR)_{24}$ cluster is elongated and composed of a Au_{23} core covered by six dimeric (SR)-Au-(SR)-Au-(SR) and three monomeric (SR)-Au-(SR) units (Scheme 1).[12] The latter are found at the equator of the cluster, whereas two sets of three dimeric units cap the poles of the cluster. These long units form two propeller-like chiral structures with identical handedness, which leads to a chiral Au−S framework. The two enantiomers of the cluster can be separated using HPLC.[29] Scheme 1 shows the structure of the anticlockwise enantiomer of $Au_{38}(SR)_{24}$ (*A*-$Au_{38}(SR)_{24}$). Due to symmetry reasons the cluster contains only four unique sites, marked a−d in Scheme 1, three on the dimeric units and one on the monomeric units. As a consequence, for a mixed cluster of composition $Au_{38}(SR)_{23}(SR')_1$ four different isomers (regioisomers) are possible corresponding to exchanges at the positions marked in Scheme 1. All these species have a reduced symmetry of C_1. Therefore, for each of these species there are 23 distinguishable positions for a second exchange, which leads to a total of 4 × 23/2 = 46 isomers with composition $Au_{38}(SR)_{22}(SR')_2$. The number of possible isomers is even larger for higher exchange species. Importantly, the discussion above refers to distinguishable isomers. Whether a certain isomer is formed depends on the kinetics of the ligand exchange for the different sites and possibly postexchange rearrangements within the ligand shell. These issues are addressed in the present study.

Here we studied ligand exchange on $Au_{38}(2\text{-PET})_{24}$ by using planar chiral monothiol **1** (PCP-4-SH, Scheme 2) derived from [2.2]paracyclophane. We find several peaks in the HPLC chromatogram although mass spectrometry shows only one compound of composition $Au_{38}(2\text{-PET})_{23}(PCP\text{-}4\text{-}S)_1$ besides the parent unexchanged $Au_{38}(2\text{-PET})_{24}$ cluster. The results show that at least three out of the four symmetry unique thiolates exchange to a significant extent at the initial stage of the reaction. Further experiments show that the ligands can migrate between different unique sites.

Scheme 1. Top: Structure of *A*-$Au_{38}(2\text{-PET})_{24}$[a]; Bottom: Structure of 2-Phenylethanethiol (2-PET)

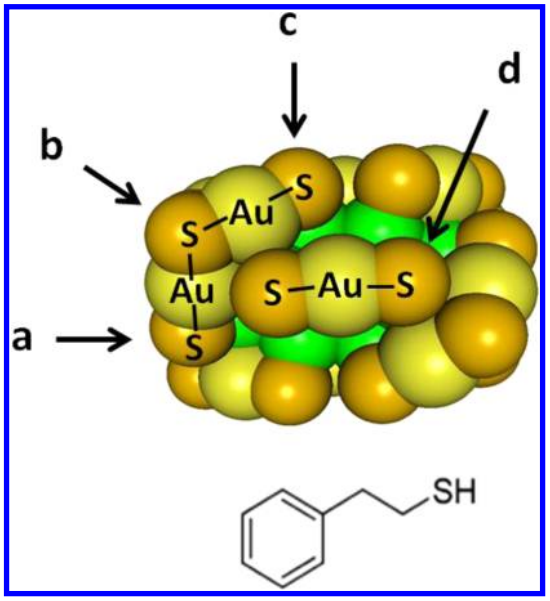

[a]Only Au and S atoms are shown. The arrows point to the four distinguishable sites on the cluster. Green: Au atoms in the core, yellow: surface Au atoms, orange: sulfur atoms. Monomeric (S−Au−S) and dimeric (S−Au−S−Au−S) units are marked.

Scheme 2. Structure of the Two Enantiomers of [2.2]Paracyclophane-4-thiol 1 (PCP-4-SH) and Their Precursors 2

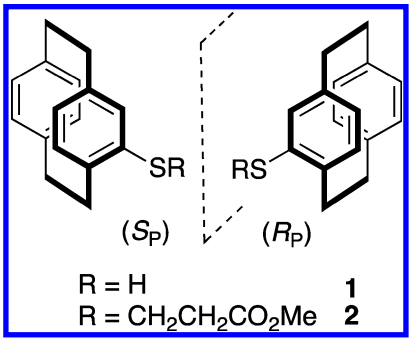

EXPERIMENTAL SECTION

Materials. All chemicals were purchased from commercial sources and used as received, if not mentioned otherwise. Nanopure water (>18 MΩ·cm) was used. Details can be found in the Supporting Information (SI).

Preparation of $Au_{38}(2\text{-PET})_{24}$. Pure $Au_{38}(2\text{-PET})_{24}$ was prepared according to published procedures.[24] Briefly, to a methanolic solution of $HAuCl_4$ a solution of L-glutathione in water was added and the reaction mixture was stirred at 0 °C. A white cloudy suspension was formed to which a $NaBH_4$ solution was added. The resulting black precipitate was collected by centrifugation and washed with methanol. Next, the precipitate was dissolved in a certain volume of water, acetone, and 2-phenylethanethiol followed by stirring at 80 °C for 3 h. The phases were separated and the residual material was copiously washed with methanol to eliminate the free thiol.

Size-exclusion chromatography (SEC) was used to separate the $Au_{38}(2\text{-PET})_{24}$ cluster from other clusters, notably $Au_{40}(2\text{-PET})_{24}$.[30] Briefly, the as-prepared clusters were passed through a BioRad BioBeads S-X1 column (1.0 m length and 2 cm in diameter) where THF was used as an eluting solvent. A number

dx.doi.org/10.1021/jp408455x | J. Phys. Chem. C 2013, 117, 21619−21625

of fractions was collected and a series of steps was run individually for each fraction until a decent degree of clusters monodispersity was reached. The isolated monodisperse gold clusters were washed by several precipitation/dispersion cycles as reported earlier.[30] The purity of the racemic $Au_{38}(2\text{-PET})_{24}$ cluster was verified by UV−vis spectroscopy, mass spectrometry, and HPLC (Phenomenex chiral column, Lux-Cellulose-1 (cellulose tris(3,5-dimethylphenylcarbamate) 5 μm, 250 × 4.6 mm), see Figure S1 in Supporting Information).

Access to Both Enantiomers of [2.2]Paracyclophane-4-thiol 1. As an extension to the synthesis of racemic [2.2]paracyclophane-4-thiol (±)-**1** we previously reported,[31] both enantiomers were obtained in high enantiomeric purities [100 and 92% ee, respectively, for (R_P)-**1** and (S_P)-**1**] by an original and efficient resolution process.[32,33] It consists of the enantioseparation of the intermediate sulfanyl ester (±)-**2** on semipreparative HPLC (1.3 g scale) with a chiral stationary phase (Chiralpak Daicel IA column), followed by a retro-Michael reaction initiated by a base and an acidic quench (see Supporting Information).

Characterization. UV−vis spectra were recorded on a Varian Cary 50 spectrometer, (path length 2 mm, CH_2Cl_2). CD spectra were recorded on a JASCO J-815 spectrometer (path length 5 mm, CH_2Cl_2); six scans were averaged. Mass spectra were recorded on a Bruker Autoflex mass spectrometer equipped with a nitrogen laser at near-threshold laser intensity in positive linear mode using DCTB as the matrix.[22]

HPLC. Separation and analysis of cluster compounds (regioisomers) were conducted on a JASCO 20xx series HPLC system equipped with a semipreparative Phenomenex Lux-Cellulose-1 column (5 μm, 250 × 10 mm) and an analytical Phenomenex Lux-Cellulose-1 column (5 μm, 250 × 4.6 mm). The detection was performed with a JASCO 2070 plus UV−vis detector at a detection wavelength of 630 nm. The samples were injected in toluene and eluted with *n*-hexane/2-propanol (more details available in SI).

Larger amounts of the enantiomers of the $Au_{38}(2\text{-PET})_{24}$ cluster were collected and dried by rotary evaporation while keeping the temperature below 25 °C to avoid racemization before further use.

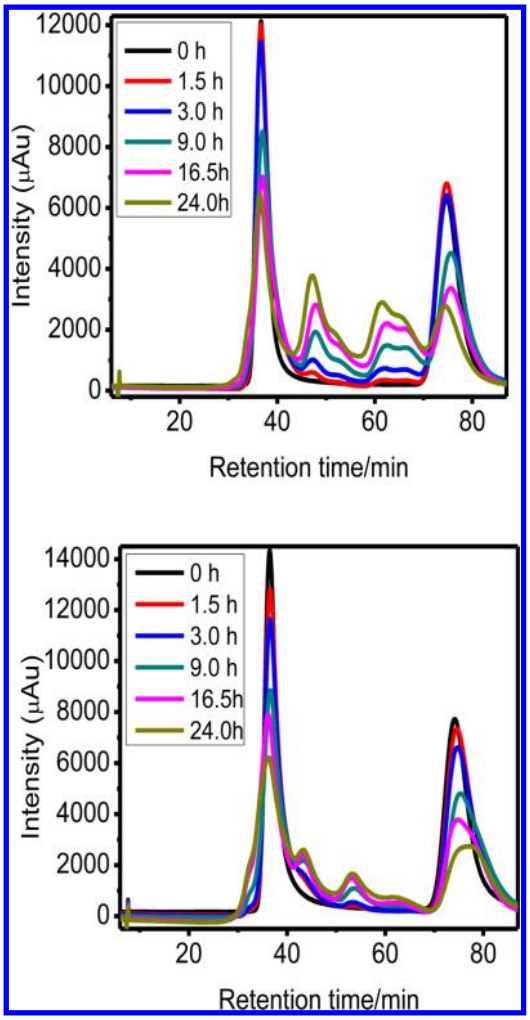

Figure 1. Chromatograms recorded in situ during ligand exchange reaction between $Au_{38}(2\text{-PET})_{24}$ and thiol **1** as a function of time. (Top) Reaction with (R_P)-**1**. (Bottom) Reaction with (S_P)-**1**. The dominant peaks at 36.83 and 75.10 min elution time correspond to the two enantiomers of the parent $Au_{38}(2\text{-PET})_{24}$ (unexchanged) cluster.

RESULTS AND DISCUSSION

The preparation of $Au_{38}(2\text{-PET})_{24}$ was performed as reported before.[24,30] UV−vis and MALDI mass spectra confirmed the successful preparation. With the pure $Au_{38}(2\text{-PET})_{24}$ in hand, the ligand exchange was first tried ex situ and analyzed by HPLC and CD spectroscopy. The development of CD signals confirmed the successful ligand exchange (see Figure S2 in Supporting Information). The reaction was then followed in situ by HPLC. For this 0.30 mg of enantiopure ligand **1** was added to a solution of 2.0 mg *rac*-$Au_{38}(2\text{-PET})_{24}$ in 1.75 mL of toluene. Figure 1 shows chromatograms recorded at different times after addition of the incoming ligand. Several peaks develop with time, which we assign to ligand exchange products. Note that in this experiment we used a racemic mixture of $Au_{38}(2\text{-PET})_{24}$ but a single enantiomer of the incoming ligand, with either (R_P) or (S_P) configuration. As a consequence for each adsorption isomer (regioisomer) two diastereomers can be formed (with the *A*- and *C*-enantiomers of the cluster, respectively).

Several peaks start to grow right after addition of the incoming thiol. This indicates that these peaks belong to $Au_{38}(2\text{-PET})_{23}(PCP\text{-}4\text{-}S)_1$ clusters because higher exchange products are expected to form with a time lag. At longer exchange times the shape of the chromatograms changes qualitatively indicating contributions from higher exchange species. UV−vis measurements did not show large changes, indicating that the cluster is stable during the ligand exchange (see Figure S3 in Supporting Information). Note that the two graphs in Figure 1 correspond to two separate experiments where the racemic cluster was reacted with (R_P)-**1** and (S_P)-**1**, respectively. Therefore, each peak in the top graph has a corresponding (enantiomer) peak in the bottom graph. Because a chiral column was used, the retention times of these enantiomeric species are not the same and it is difficult to assign the corresponding peaks. In the following we will focus only on experiments with (R_P)-**1**.

As outlined in the introduction, the number of regioisomers is very large for more than one ligand exchange. We therefore performed an experiment where the exchange reaction was quenched after a short time. In a typical reaction, *rac*-$Au_{38}(2\text{-PET})_{24}$ and thiol **1** in a molar ratio 1:6.7 in methylene chloride was stirred at room temperature for 2 h (for more details, see Supporting Information). The process was then terminated by quickly evaporating the organic solvent and washing the residue

dx.doi.org/10.1021/jp408455x | J. Phys. Chem. C 2013, 117, 21619−21625

with a mixture of methanol and acetone. The sample was then analyzed by MALDI mass spectrometry and HPLC. MALDI mass spectrometry (Figure 2) shows that the sample contains

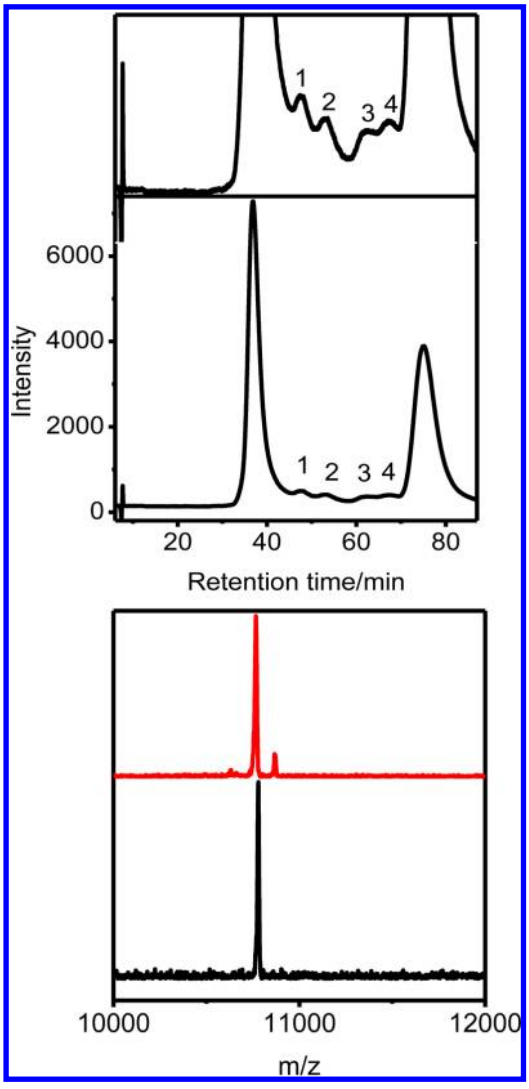

Figure 2. (Bottom) MALDI mass spectra of (black) $Au_{38}(2\text{-PET})_{24}$ and (red) after 2 h of exchange with (R_p)-**1**. The parental peak of $Au_{38}(2\text{-PET})_{24}$ clusters shows a signal at 10780 m/z (calcd 10778) and the mass signal for $Au_{38}(2\text{-PET})_{23}[(R_p)\text{-PCP-4-S}]_1$ appeared at 10881 m/z (calcd 10880). The difference between the two masses corresponds to the mass difference of the two ligands (2-PET and **1**). (Top) HPLC chromatogram of the corresponding sample after 2 h ligand exchange. The two traces correspond to the same chromatogram. The upper trace is scaled to see the small peaks.

mostly unexchanged $Au_{38}(2\text{-PET})_{24}$ (signal at 10780 Da, calculated: 10778 Da) and a small fraction (ca. 12.6%) of $Au_{38}(2\text{-PET})_{23}[(R_p)\text{-PCP-4-S}]_1$ (signal at 10881 Da, calculated 10880 Da) with one ligand exchanged. No doubly exchanged species $Au_{38}(2\text{-PET})_{22}[(R_p)\text{-PCP-4-S}]_2$ are detectable. The same sample shows several distinguishable peaks in the HPLC (at 47.44, 52.72, 62.12, and 65.96 min) for ligand exchange with (R_p)-**1** besides the two dominant signals from the parent (unexchanged) enantiomers of $Au_{38}(2\text{-PET})_{24}$ (at 36.83 and 75.10 min).

From Figure 2 we can identify at least four species with composition $Au_{38}(2\text{-PET})_{23}(PCP\text{-4-S})_1$ (labeled in Figure 2). We assign these species to regioisomers differing in the position of the exchanged ligand and the handedness of the Au−S framework. To assign these peaks to the two possible configurations of the cluster (*A* and *C*, anticlockwise or clockwise), the enantiomers of $Au_{38}(2\text{-PET})_{24}$ were separated by collecting the respective fractions in several HPLC runs.[29] The ligand exchange was then repeated with the separated enantiomers, as shown in Figure 3. This experiment reveals that

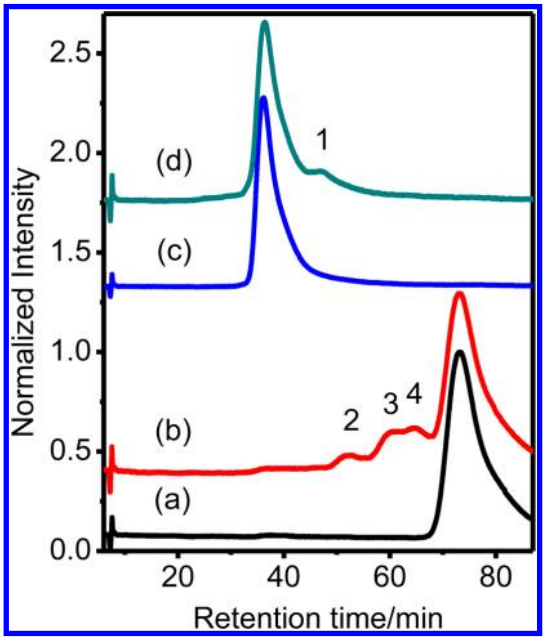

Figure 3. Chromatograms before and after ligand exchange between $Au_{38}(2\text{-PET})_{24}$ separated enantiomers and (R_p)-**1** ligand. (a) *C*-$Au_{38}(2\text{-PET})_{24}$ (enantiomer 2) before ligand exchange, (b) after ligand exchange with (R_p)-**1**, (c) *A*-$Au_{38}(2\text{-PET})_{24}$ (enantiomer 1) before ligand exchange, (d) after ligand exchange with (R_p)-**1**.

peaks at 52.72 (peak 2), 62.12 (peak 3), and 65.96 min (peak 4) are associated with the *C* configuration, whereas the peak at 47.44 min (peak 1) belongs to the *A* configuration of the cluster. (For assignment of handedness, see ref 29.) Note that additional peaks may be masked by the dominant peak of the parent (unexchanged) cluster.

We also noted that after longer exchange times additional peaks were growing in, which we assign to higher exchange species (see Figure S4 in SI).

From the experiments described above we can conclude the following: First of all, it is shown that isomers differing in the position of the exchanged ligand can be separated by HPLC. Second, the experiments show that initially exchanged ligands appear at least at three out of the four symmetry-unique sites of the $Au_{38}(2\text{-PET})_{24}$ cluster. (We cannot exclude overlap of bands such that maybe even all four sites are concerned.) Possibly the thiolate in position b (see Scheme 1) is initially not exchanged because it binds to two gold adatoms in contrast to thiolates at positions a, c, and d, which bind to one core gold atom and one gold adatom. However, at this moment this is only speculation, because the HPLC and MALDI experiments do not allow us to determine the adsorption sites.

We furthermore wondered if migration of the ligand on the cluster surface is possible. To shed light on this question the ligand exchange (for *C*-$Au_{38}(2\text{-PET})_{24}$ with (R_p)-**1**)) was performed and stopped at its initial stage in order to exclude

dx.doi.org/10.1021/jp408455x | J. Phys. Chem. C 2013, 117, 21619−21625

the formation of higher exchange products. Then one regioisomer corresponding to peak 2 (see Figures 2 and 3) was collected in several HPLC runs using a semipreparative column. Note that due to the conditions needed to exclude higher exchange products the fraction of this species in the reaction mixture is very low and therefore the amount of collected cluster is only minor. The collected regioisomer of *C*-$Au_{38}(2\text{-PET})_{23}[(R_P)\text{-PCP-4-S}]_1$ was dried and redissolved in toluene and then reinjected into the HPLC (analytical column Cellulose-1 (5 μm, 250 × 4.6 mm); for HPLC conditions, see SI). Figure 4 shows that only one dominant peak is observed in

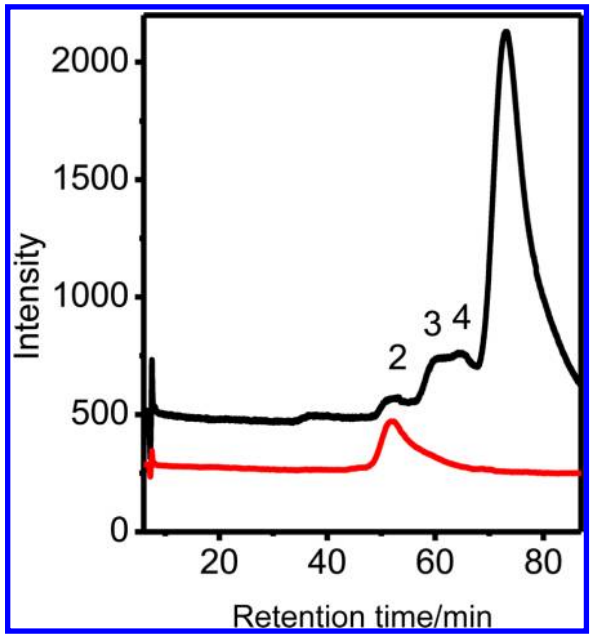

Figure 4. HPLC chromatograms of (top) *C*-$Au_{38}(2\text{-PET})_{24}$ cluster (enantiomer 2) reacted with (R_P)-**1** and (bottom) reinjected sample after collecting peak 2. The chromatograms were scaled and offset for clarity.

the chromatogram corresponding to the collected regioisomer. (A shoulder that might correspond to peak 3 is probably due to the collection process.) This experiment shows that at room temperature this regioisomer is stable at least 48 h (see also SI), that is, the corresponding ligand does not migrate to other binding sites to a significant extent.

The same sample was then heated to clarify if migration between unique sites takes place at elevated temperatures. Due to the very limited amount of sample available a systematic study at several temperatures was unfortunately not possible. Therefore the sample was first heated to 50 °C for 30 min, then to 80 °C for 30 min and finally to 80 °C for 90 min in total (Figure 5).

At 50 °C not much change is observed. However, after heating at 80 °C new peaks are seen in the HPLC chromatograms, whereas the original peak loses intensity. In Figure 6 the chromatogram after heating to 80 °C for 90 min is compared to a ligand exchange experiment with the racemic sample of the cluster. It is evident that peaks 1−4 perfectly match in the two experiments. Peaks 2−4 were assigned to different regioisomers of the *C*-$Au_{38}(2\text{-PET})_{23}[(R_P)\text{-PCP-4-S}]_1$ version of the cluster (see above). The appearance of peaks 3 and 4 demonstrates that the (R_P)-PCP-4-S ligand can migrate from the initial site of exchange to two other symmetry-unique

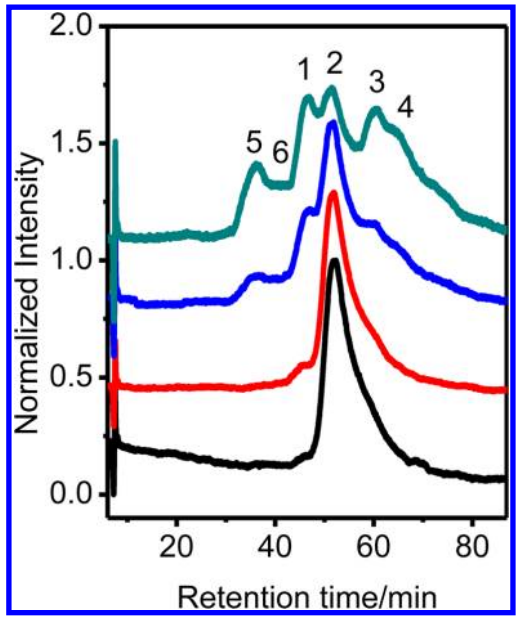

Figure 5. (Black) HPLC chromatograms of the collected peak 2 corresponding to a specific regioisomer of *C*-$Au_{38}(2\text{-PET})_{23}(R_P\text{-PCP-4-S})_1$ as collected, (red) after heating to 50 °C for 30 min, (blue) after heating to 80 °C for 30 min, and (green) after heating to 80 °C for 90 min.

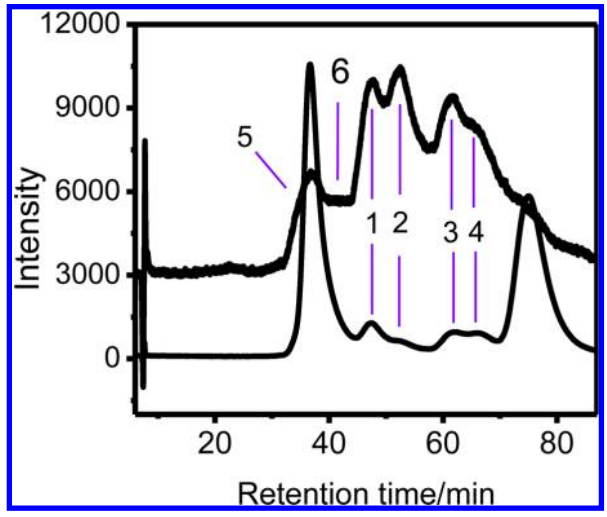

Figure 6. (Top) HPLC chromatogram of the collected peak 2 corresponding to a specific regioisomer of $Au_{38}(2\text{-PET})_{23}[(R_P)\text{-PCP-4-S}]_1$ after heating to 80 °C for 90 min. (Bottom) HPLC chromatogram of a ligand exchange reaction of racemic $Au_{38}(2\text{-PET})_{24}$ with (R_P)-**1**.

sites. There seems to be some intensity in the HPLC chromatograms at larger retention times, which may correspond to migration to the fourth possible site. Apparently the relative intensity of peaks 2−4 in the heating experiment and the ligand exchange experiment are not the same (Figure 6). This is not surprising, because one reflects the kinetics of exchange at different sites, whereas in the other experiment the distribution of sites tends toward thermodynamic equilibrium.

Evidently in the heating experiments not only peaks 3 and 4 appear, but also peak 1, which was assigned to a regioisomer of the *A*-$Au_{38}(2\text{-PET})_{23}[(R_P)\text{-PCP-4-S}]_1$ (*A*: anticlockwise) version of the cluster, thus, indicating that the cluster framework has changed handedness. We have shown before that $Au_{38}(2\text{-}$

dx.doi.org/10.1021/jp408455x | J. Phys. Chem. C 2013, 117, 21619−21625

PET)$_{24}$ racemizes at 80 °C,[27] and therefore, the appearance of regioisomers of the anticlockwise version of Au_{38}(2-PET)$_{23}$[(R_P)-PCP-4-S]$_1$ is indeed expected. Other peaks at shorter retention times (peaks 5 and 6 in Figure 6) are also assigned to regioisomers of the anticlockwise cluster. (Note: "Peak" 6 is not clearly evident as an individual peak, but from Figure 6 it is clear that there is signal between peaks 5 and 1.) These peaks were not evident in the ligand exchange experiments because they overlap with the dominant signal from the parent *A*-Au_{38}(2-PET)$_{24}$ cluster.

A final remark concerns the relative intensities of the peaks 1−6 in Figure 6. For each handedness of the cluster we observe three peaks (three regioisomers). Two of each set are more intense than the third one (intense peaks 2 and 3 and weak peak 4 for *C*-Au_{38}(2-PET)$_{23}$[(R_P)-PCP-4-S]$_1$ and intense peaks 5 and 1 and weak peak 6 for *A*-Au_{38}(2-PET)$_{23}$[(R_P)-PCP-4-S]$_1$). Even under the assumption that thermodynamic equilibrium is reached (for the distribution of the exchanged ligands over the possible sites), the relative intensity of the peaks does not need to be identical for the two versions (clockwise and anticlockwise) of the cluster because corresponding peaks are associated with diastereomers. In other words, one cannot exclude site-specific enantiodiscrimination.

CONCLUSION

When HLPC is used, it is possible to separate and isolate regioisomers arising from a mixed ligand shell. At the initial stage of ligand exchange on Au_{38}(2-PET)$_{24}$ at least three out of the four possible symmetry-unique sites are exchanged. At room temperature the exchanged thiolate does not move to other symmetry-unique sites and even heating to 50 °C for 30 min has no appreciable effect. Upon heating to 80 °C, the thiolates can migrate to other symmetry-unique sites and at the same time inversion of the Au−S framework chirality (racemization) is observed.

The results indicate that on the Au_{38}(2-PET)$_{24}$ cluster it is difficult to perform site-specific exchange with a monothiol (although other thiols than the one studied here might result in other exchange patterns). On the other hand, the observations also demonstrate that upon heating the thiolates on the cluster surface can migrate between symmetry-unique sites and therefore reach the thermodynamic most stable distribution, which might be used to prepare well-defined clusters with particular ligand distribution patterns.

ASSOCIATED CONTENT

Supporting Information

Synthesis of (R_p)-**1** and (S_p)-**1** through resolution of (±)-**2**, synthesis of *rac*-Au_{38}(2-PET)$_{24}$, details on ligand exchange experiments, UV−vis and CD spectra after exchange, HPLC method used for in situ monitoring, full spectroscopic data, and HPLC charts for **1** and **2**. This material is available free of charge via the Internet at http://pubs.acs.org.

AUTHOR INFORMATION

Corresponding Author

*E-mail: thomas.buergi@unige.ch.

Present Address

[§]Molecular Imaging and Photonics, KU Leuven, Celestijnenlaan 200D, 3001 Heverlee, Belgium (S.K.).

Notes

The authors declare no competing financial interest.

ACKNOWLEDGMENTS

We thank Dr. Igor Dolamic for help with the HPLC work and Sophie Michalet for measurement of the mass spectra. We acknowledge financial support from the Swiss National Science Foundation, the University of Geneva (T.B.), Swiss Government FCS Grant (L.B.), and the German Academic Exchange Service (S.K.). The work was also supported by EDRF fundings through the IS:CEChem Project and INTERREG IV A France-(Channel)−England Programme (Project No. 4061), both are gratefully thanked for their financial support (D.D.).

REFERENCES

(1) Hakkinen, H. The Gold−Sulfur Interface at the Nanoscale. *Nat. Chem.* **2012**, *4* (6), 443−455.

(2) Maity, P.; Xie, S. H.; Yamauchi, M.; Tsukuda, T. Stabilized Gold Clusters: From Isolation Toward Controlled Synthesis. *Nanoscale* **2012**, *4* (14), 4027−4037.

(3) Qian, H. F.; Zhu, M. Z.; Wu, Z. K.; Jin, R. C. Quantum-Sized Gold Nanoclusters with Atomic Precision. *Acc. Chem. Res.* **2012**, *45* (9), 1470−1479.

(4) Zhu, Y.; Qian, H. F.; Drake, B. A.; Jin, R. C. Atomically Precise $Au_{25}(SR)_{18}$ Nanoparticles as Catalysts for the Selective Hydrogenation of *α,β*-Unsaturated Ketones and Aldehydes. *Angew. Chem., Int. Ed.* **2010**, *49* (7), 1295−1298.

(5) Wang, M.; Wu, Z. K.; Yang, J.; Wang, G. Z.; Wang, H. Z.; Cai, W. P. $Au_{25}(SG)_{18}$ as a Fluorescent Iodide Sensor. *Nanoscale* **2012**, *4* (14), 4087−4090.

(6) Ghosh, P.; Han, G.; De, M.; Kim, C. K.; Rotello, V. M. Gold Nanoparticles in Delivery Applications. *Adv. Drug Delivery Rev.* **2008**, *60* (11), 1307−1315.

(7) Brust, M.; Walker, M.; Bethell, D.; Schiffrin, D. J.; Whyman, R. Synthesis of Thiol-Derivatized Gold Nanoparticles in a Two-Phase Liquid−Liquid System. *J. Chem. Soc., Chem. Commun.* **1994**, *7*, 801−802.

(8) Whetten, R. L.; Khoury, J. T.; Alvarez, M. M.; Murthy, S.; Vezmar, I.; Wang, Z. L.; Stephens, P. W.; Cleveland, C. L.; Luedtke, W. D.; Landman, U. Nanocrystal Gold Molecules. *Adv. Mater.* **1996**, *8* (5), 428−433.

(9) Chaki, N. K.; Negishi, Y.; Tsunoyama, H.; Shichibu, Y.; Tsukuda, T. Ubiquitous 8 and 29 kDa Gold: Alkanethiolate Cluster Compounds: Mass-Spectrometric Determination of Molecular Formulas and Structural Implications. *J. Am. Chem. Soc.* **2008**, *130* (27), 8608−8610.

(10) Jadzinsky, P. D.; Calero, G.; Ackerson, C. J.; Bushnell, D. A.; Kornberg, R. D. Structure of a Thiol Monolayer-Protected Gold Nanoparticle at 1.1 Å Resolution. *Science* **2007**, *318* (5849), 430−433.

(11) Heaven, M. W.; Dass, A.; White, P. S.; Holt, K. M.; Murray, R. W. Crystal Structure of the Gold Nanoparticle $[N(C_8H_{17})_4][Au_{25}(SCH_2CH_2Ph)_{18}]$. *J. Am. Chem. Soc.* **2008**, *130* (12), 3754−3755.

(12) Qian, H. F.; Eckenhoff, W. T.; Zhu, Y.; Pintauer, T.; Jin, R. C. Total Structure Determination of Thiolate-Protected Au_{38} Nanoparticles. *J. Am. Chem. Soc.* **2010**, *132* (24), 8280−8281.

(13) Hostetler, M. J.; Templeton, A. C.; Murray, R. W. Dynamics of Place-Exchange Reactions on Monolayer-Protected Gold Cluster Molecules. *Langmuir* **1999**, *15* (11), 3782−3789.

(14) Dass, A.; Holt, K.; Parker, J. F.; Feldberg, S. W.; Murray, R. W. Mass Spectrometrically Detected Statistical Aspects of Ligand Populations in Mixed Monolayer $Au_{25}L_{18}$ Nanoparticles. *J. Phys. Chem. C* **2008**, *112* (51), 20276−20283.

(15) Heinecke, C. L.; Ni, T. W.; Malola, S.; Makinen, V.; Wong, O. A.; Hakkinen, H.; Ackerson, C. J. Structural and Theoretical Basis for Ligand Exchange on Thiolate Monolayer Protected Gold Nanoclusters. *J. Am. Chem. Soc.* **2012**, *134* (32), 13316−13322.

(16) Cseh, L.; Mehl, G. H. The Design and Investigation of Room Temperature Thermotropic Nematic Gold Nanoparticles. *J. Am. Chem. Soc.* **2006**, *128* (41), 13376−13377.

(17) Frein, S.; Boudon, J.; Vonlanthen, M.; Scharf, T.; Barbera, J.; Suss-Fink, G.; Burgi, T.; Deschenaux, R. Liquid-Crystalline Thiol- and Disulfide-Based Dendrimers for the Functionalization of Gold Nanoparticles. *Helv. Chim. Acta* **2008**, *91* (12), 2321−2337.
(18) Basiruddin, S. K.; Saha, A.; Pradhan, N.; Jana, N. R. Advances in Coating Chemistry in Deriving Soluble Functional Nanoparticle. *J. Phys. Chem. C* **2010**, *114* (25), 11009−11017.
(19) Shibu, E. S.; Muhammed, M. A. H.; Tsukuda, T.; Pradeep, T. Ligand Exchange of $Au_{25}SG_{18}$ Leading to Functionalized Gold Clusters: Spectroscopy, Kinetics, and Luminescence. *J. Phys. Chem. C* **2008**, *112* (32), 12168−12176.
(20) Guo, R.; Song, Y.; Wang, G. L.; Murray, R. W. Does Core Size Matter in the Kinetics of Ligand Exchanges of Monolayer-Protected Au Clusters? *J. Am. Chem. Soc.* **2005**, *127* (8), 2752−2757.
(21) Song, Y.; Murray, R. W. Dynamics and Extent of Ligand Exchange Depend on Electronic Charge of Metal Nanoparticles. *J. Am. Chem. Soc.* **2002**, *124* (24), 7096−7102.
(22) Dass, A.; Stevenson, A.; Dubay, G. R.; Tracy, J. B.; Murray, R. W. Nanoparticle MALDI-TOF Mass Spectrometry Without Fragmentation: $Au_{25}(SCH_2CH_2Ph)_{18}$ and Mixed Monolayer $Au_{25}(SCH_2CH_2Ph)_{18-x}(L)x$. *J. Am. Chem. Soc.* **2008**, *130* (18), 5940−5946.
(23) Niihori, Y.; Matsuzaki, M.; Pradeep, T.; Negishi, Y. Separation of Precise Compositions of Noble Metal Clusters Protected with Mixed Ligands. *J. Am. Chem. Soc.* **2013**, *135* (13), 4946−4949.
(24) Knoppe, S.; Dharmaratne, A. C.; Schreiner, E.; Dass, A.; Burgi, T. Ligand Exchange Reactions on Au_{38} and Au_{40} Clusters: A Combined Circular Dichroism and Mass Spectrometry Study. *J. Am. Chem. Soc.* **2010**, *132* (47), 16783−16789.
(25) Tracy, J. B.; Crowe, M. C.; Parker, J. F.; Hampe, O.; Fields-Zinna, C. A.; Dass, A.; Murray, R. W. Electrospray Ionization Mass Spectrometry of Uniform and Mixed Monolayer Nanoparticles: $Au_{25}[S(CH_2)_2Ph]_{18}$ and $Au_{25}[S(CH_2)_2Ph]_{18-x}(SR)x$. *J. Am. Chem. Soc.* **2007**, *129* (51), 16209−16215.
(26) Knoppe, S.; Azoulay, R.; Dass, A.; Burgi, T. In Situ Reaction Monitoring Reveals a Diastereoselective Ligand Exchange Reaction Between the Intrinsically Chiral $Au_{38}(SR)_{24}$ and Chiral Thiols. *J. Am. Chem. Soc.* **2012**, *134* (50), 20302−20305.
(27) Knoppe, S.; Dolamic, I.; Burgi, T. Racemization of a Chiral Nanoparticle Evidences the Flexibility of the Gold-Thiolate Interface. *J. Am. Chem. Soc.* **2012**, *134* (31), 13114−13120.
(28) Knoppe, S.; Michalet, S.; Burgi, T. Stabilization of Thiolate-Protected Gold Clusters Against Thermal Inversion: Diastereomeric $Au_{38}(SCH_2CH_2Ph)_{24-2x}(R\text{-BINAS})_x$. *J. Phys. Chem. C* **2013**, *117*, 15354−15361.
(29) Dolamic, I.; Knoppe, S.; Dass, A.; Burgi, T. First Enantioseparation and Circular Dichroism Spectra of Au_{38} Clusters Protected by Achiral Ligands. *Nat. Commun.* **2012**, *3*, 798.
(30) Knoppe, S.; Boudon, J.; Dolamic, I.; Dass, A.; Burgi, T. Size Exclusion Chromatography for Semipreparative Scale Separation of $Au_{38}(SR)_{24}$ and $Au_{40}(SR)_{24}$ and Larger Clusters. *Anal. Chem.* **2011**, *83* (13), 5056−5061.
(31) Lohier, J. F.; Foucoin, F.; Jaffrès, P. A.; Garcia, J. I.; Sopkova-de Oliveira Santos, J.; Perrio, S.; Metzner, P. An Efficient and Straightforward Access to Sulfur Substituted [2.2] Paracyclophanes: Application to Stereoselective Sulfenate Salt Alkylation. *Org. Lett.* **2008**, *10* (6), 1271−1274.
(32) Rowlands, G. J.; Seacome, R. J. Enantiospecific Synthesis of [2.2] Paracyclophane-4-Thiol and Derivatives. *Beilstein J. Org. Chem.* **2009**, *5*, 9.
(33) Kreis, M.; Brase, S. A General and Efficient Method for the Synthesis of Silyl-Protected Arenethiols from Aryl Halides or Triflates. *Adv. Synth. Catal.* **2005**, *347* (2−3), 313−319.